PLOS ONE
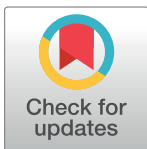
Swimming direction of the glass catfish is responsive to magnetic stimulation

Ryan D. Hunt[1,2], **Ryan C. Ashbaugh**[1,2,3], **Mark Reimers**[2,4], **Lalita Udpa**[3], **Gabriela Saldana De Jimenez**[2], **Michael Moore**[2,4], **Assaf A. Gilad**[1,5,6], **Galit Pelled**[1,2,5]*

1 Department of Biomedical Engineering, Michigan State University, East Lansing, Michigan, United States of America, 2 Neuroengineering Division, Institute for Quantitative Health Science and Engineering, Michigan State University, East Lansing, Michigan, United States of America, 3 Department of Electrical and Computer Engineering, Michigan State University, East Lansing, Michigan, United States of America, 4 Department of Physiology and Neuroscience Program, Michigan State University, East Lansing, Michigan, United States of America, 5 Department of Radiology, Michigan State University, East Lansing, Michigan, United States of America, 6 Synthetic Biology Division, Institute for Quantitative Health Science and Engineering, Michigan State University, East Lansing, Michigan, United States of America

* Pelledga@msu.edu

Abstract

Several marine species have developed a magnetic perception that is essential for navigation and detection of prey and predators. One of these species is the transparent glass catfish that contains an ampullary organ dedicated to sense magnetic fields. Here we examine the behavior of the glass catfish in response to static magnetic fields which will provide valuable insight on function of this magnetic response. By utilizing state of the art animal tracking software and artificial intelligence approaches, we quantified the effects of magnetic fields on the swimming direction of glass catfish. The results demonstrate that glass catfish placed in a radial arm maze, consistently swim away from magnetic fields over 20 µT and show adaptability to changing magnetic field direction and location.

Introduction

Throughout evolution, organisms have developed unique strategies to become more competitive in their environment. One unique adaptation is the ability to sense magnetic fields, i.e., magnetoreception. While animals like salmonids, pigeons, eels and sea turtles use magnetoreception to migrate over thousands of kilometers [1–10], non-migratory fish species have also shown evidence of magnetoreception [11, 12]. The glass catfish is also known to be sensitive to the Earth's magnetic field [13, 14].

The glass catfish (*Kryptopterus vitreolus*) is found in slow moving fresh water in Southeast Asia, ranges from 31.4–64.6 mm in length and is transparent except for their organ packed head [15]. The glass catfish has historically been of interest to a wide range of scientific disciplines, including circulation [16], cell line establishment [17] and electroreception [18, 19]. The interest in this species' magnetoreception has recently been reignited due to its potential to be part of a synthetic system that will allow remote, magnetic control, of neural function [20].

New advances in molecular biology have brought new tools to identify the mechanisms by which this species respond to electromagnetic fields. Recently, we have discovered a gene (electromagnetic perceptive gene (EPG)) that is expressed in the glass catfish's ampullary organ and is specifically activated in response to magnetic stimuli. This genetic-based magnetoreception has a great potential as a neuromodulation technology and as a valuable tool to study neural behavior from the molecular to network levels [20–22]. However, the mechanism by which magnetoreception manifests and functions is not well understood [23–29].

This work was designed to characterize the natural behavior of glass catfish in response to magnetic fields. This understanding may lead to improved engineering of magnetic-receptive modulation and sets a foundation for a new magnetically sensitive animal model. We capitalized on new concepts of artificial intelligence as well as traditional video tracking algorithms to quantify how glass catfish respond to magnetic stimulation with high spatial and temporal resolution.

Methods

All animal procedures were conducted in accordance with the NIH Guide for the Care and Use of Laboratory Animals and approved by the Michigan State University Institutional Animal Care and Use Committee.

Thirteen Glass catfish of undetermined sex and age [30] were imported from Thailand to the United States and housed in a standard 30-gallon fish tank with a 12-hour day/night cycle with water maintained at 27 degrees and provided with an enriched environment. After arriving from Thailand, fish were acclimatized for 6 weeks before starting experiments. Water quality was checked daily for ammonium, nitrite, and nitrate. Fish were fed a diet of fresh hatched brine shrimp twice per day. All experiments were conducted between the hours of 11 am and 4 pm to eliminate behavioral changes due to feeding [31] and light cycle.

The Y-maze's arms were 60 cm long and 10 cm wide with a central area of 10x10x10 cm (AnyMaze, San Diego Instruments, CA). One week prior to starting experiments all fish were transitioned from their tanks to the radial Y-maze where they lived for the duration of each experiment (2 weeks). Enrichment materials were carried over from permanent housing to Y-maze, rearranged daily and removed prior to starting experiments. A five-gallon water change was done weekly in the Y-maze with mature water to control water quality and reduce the impact of any unknown pheromones. The same fish were used for all experiments, thirteen fish were tested in constant location and twelve in alternating location experiment. The magnetic stimulus and the sham stimulus were placed 10 cm from the end of an arm, inside of the maze. Each trial was recorded for 30 minutes by overhead cameras while the experimenter was out of the room. Each trial was repeated four times for each condition for a total of 24 trials. In order to negate the effects of Earth's intrinsic magnetic field, the location of the magnet was rotated during the changing location experiment: Arm 1 was oriented in the south west direction, Arm 2 in the northern direction and Arm 3 in the south east direction.

A permanent Neodymium Rare Earth Magnet (11.5 cm x 3.18 cm x 2.2 cm) with a horizontal magnetic flux of 577 mT at the magnet's surface was placed 10 cm from the end of one of the Y-maze arms. The strength of the magnetic field induced by the magnet was calculated by COMSOL (Fig 1). A sham stimulus was made from plastic and aluminum foil, with similar dimensions to the magnet. All recordings were analyzed by a radial-maze tracking software written in Matlab by Delcourt *et al*. [32]. Delcourt *et al*. software is available on github:: https://github.com/sjmgarnier/projectRadial. Videos were taken originally in AnyMaze format and converted to.mp4. The Matlab program then created a background image by taking an average of 100 frames. Fish location was determined by subtracting the background image
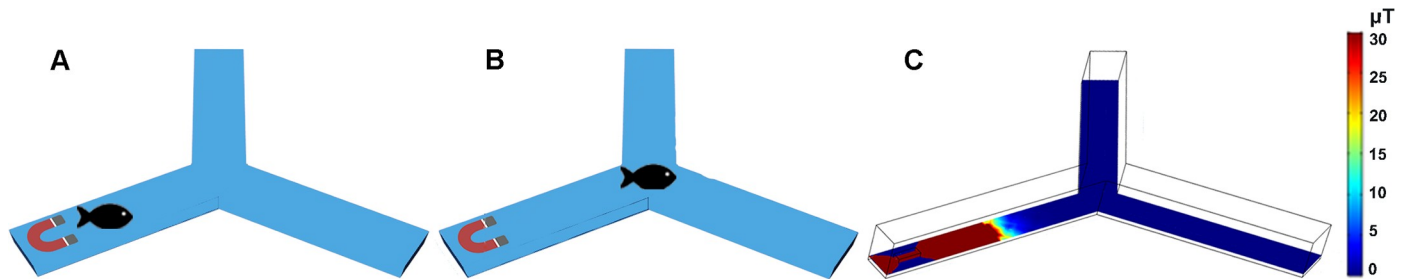
Fig 1. Diagram of the experimental set up. A) Constant location of stimulus-The magnet was always placed in the same arm and the fish were barricaded randomly in one of the three arms. **B)** Changing location of stimulus- The magnet was randomly placed in one of the three arms, and fish were always barricaded in the center of the Y-maze. **C)** COSMOL stimulation depicting the strength of the magnetic field induced by the magnet.

from each frame, remaining pixels with a grey scale value higher than threshold were given a value of 1, continuous pixels with a value of 1 were labeled as a fish. The spatial resolution of all videos was 3.57 ± .52 pixels/cm and were recorded at 30 frames per second. The number of fish in each arm was reported every second, however fish located in the center of the Y-maze were not reported. The average of the 4 trials for the arm of interest (Magnet/Sham) and the pooled average of the two empty arms (No Magnet/Sham) is reported in Figs 2 and 3.

Data is reported as median ± 95% confidence intervals (CI). Data was analyzed in R Studio, using the bootstrap method to calculate CI's and Mann-Whitney U Test to compare the arm of interest with the pooled average of the two empty arms across the 4 trials. Shapiro-Wilke tests and Q-Q plot analysis were used to determine distribution of the data which was found to be not normally distributed.

In a separate set of experiments, a single fish was selected from the school and placed in the center of the Y-maze. Two trials of magnet and sham conditions were conducted: one set of trials was used for computer training, and the other for analysis using the trained software. DeepLabCut [33, 34] was used to track the location of a single fish in the Y-maze. DeepLabCut code is available at the following address: https://github.com/DeepLabCut/DeepLabCut.git. The program was initially trained on 20 frames and ran through 1,300,000 iterations. After initial training, outlier frames were extracted and re-labeled. The program was re-trained with the addition of the outlier frames for 100,000 iterations. Retraining was done three times until visual inspection and expected error were satisfactory (±15 pixels). DeepLabCut results were extracted using an output CSV file from the code, which provides the x,y coordinates of the tracked fish for every frame of the video. This file was exported to R-Studio and plotted as a standard scatter plot and overlaid on a Y-maze diagram. Tracked videos are two minutes and fifty seconds long (5,100 frames).

Results

Constant location of stimulus

We characterized fish behavior as a response to a magnetic stimulation that was consistently present at the same location. In these sets of experiments the magnet was always placed in Arm 1 of the Y-maze. The initial location of the fish school (n = 13) was changed randomly to one of the Y-maze's three arms. Each trial was repeated four times for each arm for a total of 24 trials. The number of fish present in Arm 1 (Arm with magnet) was significantly lower than the number of fish in the other two arms in the first minute (Arm 1-Magnet, 7.69% ± 8.4%; Arm 2 & 3-No Magnet, 38.46% ± 8.84%; P = < .0005, U = 147424, Mann-Whitney U Test), after 5 minutes (Arm 1-Magnet, 7.69% ± 2.3%; Arm 2 & 3-No Magnet, 38.46% ± 6.41%; P = <
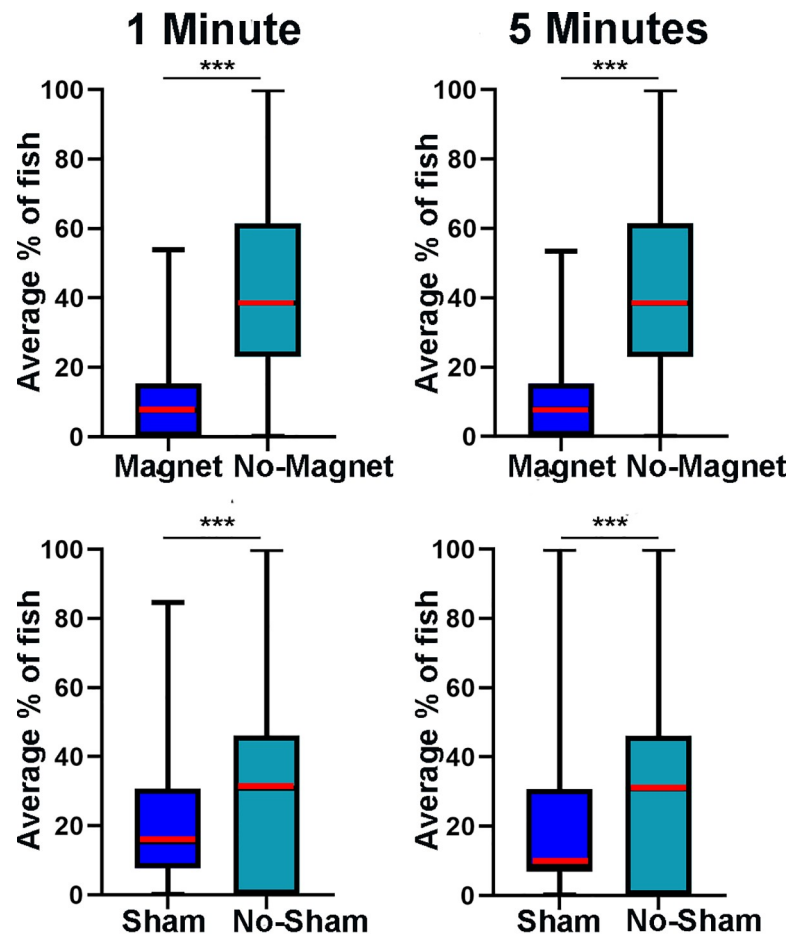
1 Minute   5 Minutes

Fig 2. Constant location of stimulus results. The average percentage of the fish school (n = 13) in sham/magnet (Arm 1) compared to the merged data from no-sham/magnet arms (Arm 2 & 3). There is significantly less fish in the arm with magnet present compared to the pooled no-magnet arms on average. There is also significantly more fish in the no-sham arms compared to sham arm (*** = p < .0005, Mann-Whitney U Test). This is a Spear Box Plot with the box showing 25% to 75% interquartile range and median represented as a red line, whiskers show minimum and maximum values. **Magnet 1 minute:** median = 7.69%, IQR = 15.39%; **No Magnet 1 Minute:** median = 38.46%, IQR = 38.46%; **Magnet 5 minutes:** median = 7.79%, IQR = 15.39%; **No Magnet 5 Minutes:** median = 38.46%, IQR = 38.46%; **Sham 1 minute:** median = 15.39%, IQR = 23.08%; **No Sham 1 minute:** median = 30.77%, IQR = 46.15%; **Sham 5 minutes:** median = 7.69%, IQR = 23.08%; **No Sham 5 minutes:** median = 30.77%, IQR = 46.15%.

https://doi.org/10.1371/journal.pone.0248141.g002

.0005, U = 3227686, Mann-Whitney U Test), and over the entire recording that lasted 30 minutes (Arm 1-Magnet, 7.69% ± 1%; Arm 2 & 3-No Magnet, 38.46% ± 3%; P = < .0005, U = 175417129, Mann-Whitney U Test) ([Fig 2](#)). When the initial fish location was also in Arm 1, the school immediately swam away from that arm and stayed away. In contrast, when the sham stimulus was placed in Arm 1, the fish exhibited less preference for the no-sham arms than they did in the previous experiment, after 1 minute, (Arm 1-Sham, 15.39% ± 8.4%; Arm 2 & 3-No Sham, 30.77% ± 15.94%; P = < .0005, U = 416993 Mann-Whitney U Test,), after 5 minutes, (Arm 1-Sham, 7.69% ± 4.75%; Arm 2 & 3-No Sham, 30.77% ± 5.58%; P = < .0005, U = 9618087, Mann-Whitney U Test), and after 30 minutes, (Arm 1-Sham, 7.69% ± 2.08%; Arm 2 & 3-No Sham, 38.46% ± 3.23%; P = < .005, U = 3.12E8 Mann-Whitney U Test). Between experiments it was also observed that there is significantly less fish in Arm 1 when the
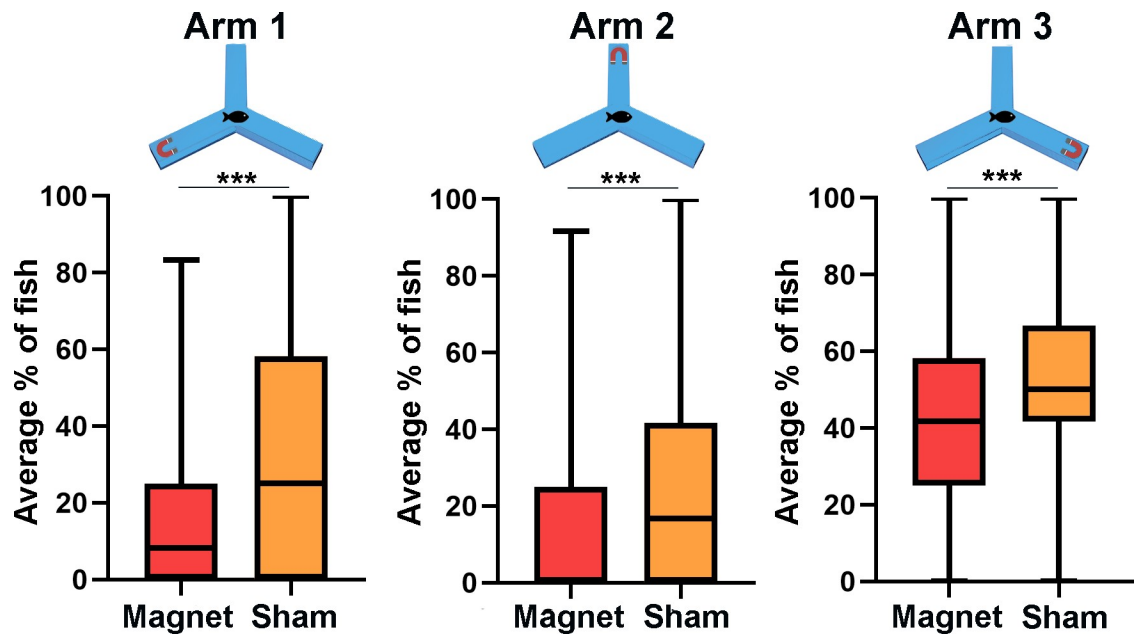
Fig 3. Changing location of stimulus results. The average percentage of fish school (n = 12) in each arm over five minutes. There is significantly less fish, on average, in the arm when magnet is present compared to when sham in present in the same arm (*** p < .0005 Mann-Whitney U Test). This is a Spear Box Plot with the box showing 25% to 75% interquartile range and median represented as a black line, whiskers show minimum and maximum values. **Arm 1 Magnet:** median = 8.33%, IQR = 25%; **Arm 1 Sham:** median = 25%, IQR = 58.77%; **Arm 2 Magnet:** median = 0%, IQR = 25%; **Arm 2 Sham:** median = 16.67%, IQR = 41.67%; **Arm 3 Magnet:** median = 41.67%, IQR = 33.33%; **Arm 3 Sham:** median = 50%, IQR = 25%.

https://doi.org/10.1371/journal.pone.0248141.g003

magnet is present compared to when the sham is present at all time points (p < .0005, Mann-Whitney U Test). These experiments showed that glass catfish prefer to avoid swimming in water with a magnetic strength over 20 µT (Figs 1c and 2). Results indicate that regardless of the initial location of the fish, they tend to avoid Arm 1 more when magnet was present compared to sham at all time points (p < .0005,Mann-Whitney U Test).

Changing location of stimulus

We then sought to determine if fish behavior changed with the location of the magnetic stimulation. In this set of experiments the fish school (n = 12) was barricaded in the middle of the Y-maze, and the magnetic or sham stimuli were placed randomly in one of the arms (Fig 1b). After barricade removal the fish swam away from the magnet and explored the two other maze-arms. In line with previous experiments, there are significantly less fish present in the arm on average when the magnet was present compared to when the sham stimulus was present (Arm 1-Magnet, 8.33% ± 8.25%, Arm 1-Sham, 25% ± 15.68%, U = 908254; Arm 2-Magnet, 11.53% ± 9.71%, Arm 2-Sham, 16.67% ± 23.4%, U = 890468; Arm 3-Magnet, 41.67% ± 22.6%; Arm 3-Sham, 50% ± 5.11%, U = 983677; P = < .0005 Mann-Whitney U Test for all tests). Fig 3 shows the average percentage of the fish school present in each arm within the first 5 minutes of recording.

For the purpose of individual swim pattern analysis, one fish was placed in the middle of the Y-maze. Once the barricade had been removed the fish swam across two arms where no magnet was present but exhibited a clear avoidance from the arm containing the magnet. We used a state-of-the-art artificial intelligence (AI) approach, DeepLabCut [33, 34] to track the fish's swimming path. DeepLabCut was successfully trained on a single fish with an error of
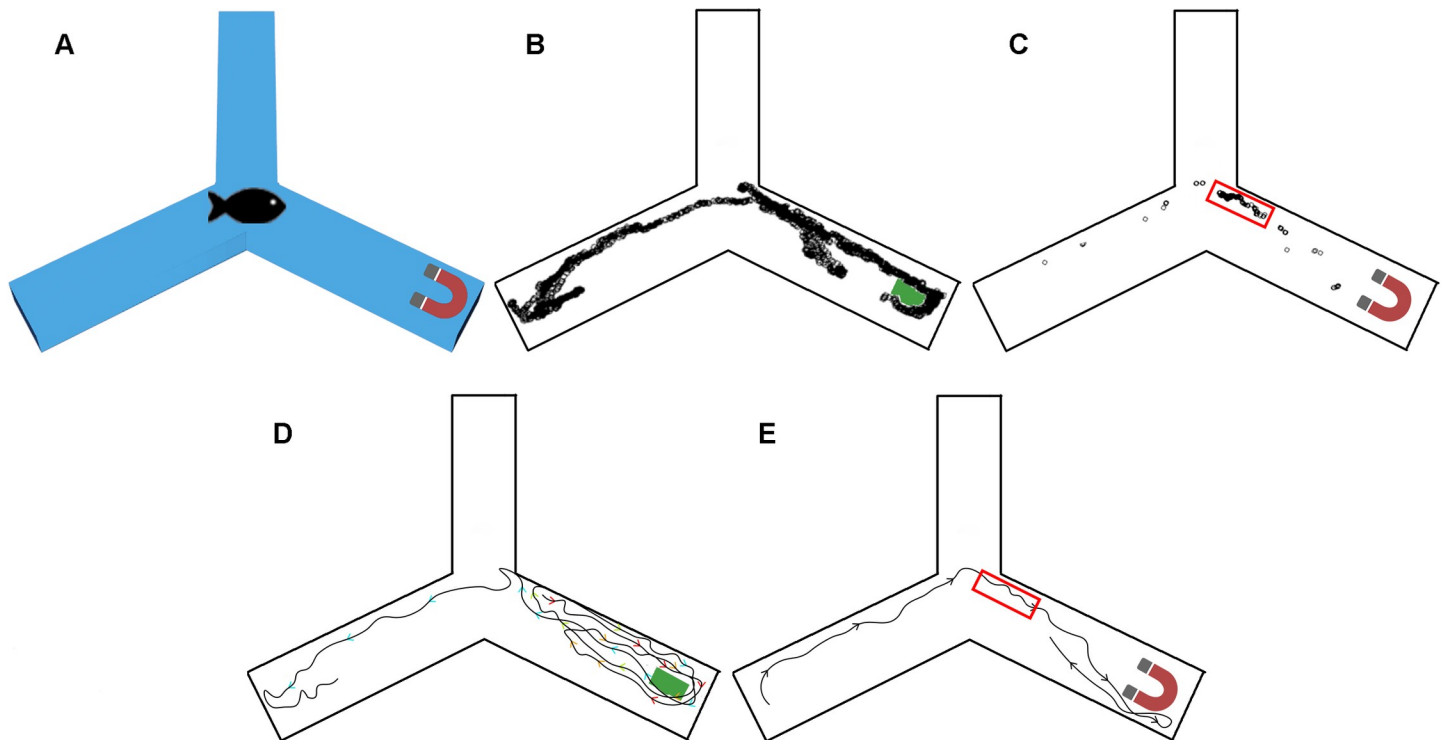
Fig 4. DeepLabCut tracking of a single fish. A) Experimental set up. **B)** Sham, **C)** Magnet. The fish position is shown here over every frame for 170 s (5,100 frames). Indivudual values were exported and plotted using R and overlaid on a Y-maze diagram. **D)** Directional tracing of sham experiment. **E)** Directional tracing of magnet experiment. The red box on **B** and **E** represents the area where the fish spent 77% (131 seconds) of its time during the magnetic trial. The movment down the two arms were rapid, resulting in less total visible dots.

less than 4.2 cm or 15 pixels. Fig 4 shows that magnetic stimulation results in an individual fish swimming away from the magnet immediately after barricade removal. Consistent with previous results, sham stimulus did not induce an avoidance behavior.

Discussion

Several marine species have developed a magnetic perception that is useful in navigation and the detection of prey and predators [6, 35], for review see [36–38]; animals such as sharks and platypus, use magnetoreception for prey detection [39–43]. Others, like ants [44], use this sense for predator avoidance and the nematode, *Caenorhabditis elegance* uses magnetoreception for vertical navigation in soil [45]. Even cattle have been shown to align themselves with electromagnetic pulses [46]. Recently, evidence of magnetoreception has been unveiled in fish species previously thought to me non-magnetic, such as zebrafish [47]. The glass catfish is a transparent fish found in slow moving rivers of Southeast Asia where visibility is low [15, 17]. Until recently, the transparent glass catfish was commonly identified as *Kryptopterus bicirrhis* but is now known to be *Kryptopterus vitreolus* [15]. It appears plausible that in these types of conditions, magnetic perception is an advantageous trait to conserve. However, the mechanisms allowing magnetic sensation remain largely unknown [26, 38]. We have used state-of-the-art software based on artificial intelligence object tracking algorithms to characterize glass catfish behavioral response to magnetic fields. The results indicate that glass catfish consistently swim away from magnetic fields over 20 μT and show adaptability to changing magnetic field direction and location. In addition, our results show that this magnetic avoidance

behavior is not influenced by school behavior. It is important to note that there is significantly less fish in the Sham arm compared to No-Sham arm in the constant location stimulus experiment. We hypothesize that this is because the fish developed an avoidance for Arm 1 due to repeatedly exposed to the magnet. In the alternating location experiment we see no avoidance of the sham object in all three arms.

We have previously demonstrated that the modulatory effects of magnetic stimulation on mammalian cells transfected with EPG was induced by magnetic fields of 50 mT [21]. However, in this experiment we see that fish are significantly more sensitive to magnetic fields than transfected cells, with fish starting to exhibit avoidance behavior at ~20 µT (Figs 2 and 3). While the pathway by which EPG modulates calcium channels is unknown [20, 21] it is possible that there are accessory proteins that are currently remain unknown, which amplify magnetic sensitivity in glass catfish. It could also be possible that different cellular mechanisms occur over the time when EPG is exposed to magnetic fields. Currently, we can only evoke a cellular response by using strong magnetic fields in culture (> 50mT). However, the Earth's magnetic field is only 30 µT-60 µT, and yet, is readily detected by glass catfish. One of the major challenges in EPG's development as a neuromodulatory technology is the attenuation of magnetic fields over distance. If the biological amplification properties of the glass catfish are uncovered, this technology could be used to treat deep brain afflictions without the need for surgery.

Using AI such as DeepLabCut can be transformative to animal behavior studies. Using this method, we could follow the swimming pattern of an individual fish, over thousands of frames with high spatial and temporal resolution. Another advantage is the machine learning components of AI. The more trials run through DeepLabCut, the more efficient and accurate it becomes at tracing animals in similar situations. However, the transparency of glass catfish caused detection difficulties with DeepLabCut and recording hardware when rapid movement caused insufficient contrast between the fish and Y-maze. In Fig 4B, during the sham stimulus the fish swam at a gradual pace throughout the maze. However, during magnetic stimulus the fish tend to stay in one area then dash to the end of an arm and back. During these rapids movements our recording software experienced a drop in frame rate Once the fish slowed down and the contrast was restored, the tracking became accurate. While the transparent glass catfish poise unique challenges for AI tracing due to its transparent body, this AI tracing approach can be beneficial to track movement of other marine species.

We have established that the glass catfish has unique magnetic field sensing capabilities that position it as a valuable model to study magnetoreception in animal species. The cellular mechanisms allowing this capability remains to be determined. We have already identified and cloned the EPG from glass catfish. But is this the only magnetic-sensitive protein? Does it work with other proteins to amplify and modulate its activity? Do other animal species that have been shown to be sensitive to magnetic fields have similar proteins? This animal model can provide key information to address these questions. By characterizing the behavior of glass catfish, we are now working towards developing a fish with a knock-out in the EPG gene. This will elucidate if there are additional genes associated with magnetic responses and will facilitate the development of the next generation of additional magnetic sensing molecular tools.

Author Contributions

Conceptualization: Ryan D. Hunt, Galit Pelled.

Data curation: Ryan D. Hunt, Ryan C. Ashbaugh.

References

1. Henrik M. Long-distance navigation and magnetoreception in migratory animals. Nature; London. 2018; 558(7708):50–9.

2. Wynn J, Padget O, Mouritsen H, Perrins C, Guilford T. Natal imprinting to the Earth's magnetic field in a pelagic seabird. Current Biology. 2020; 30(14):2869–73.e2. https://doi.org/10.1016/j.cub.2020.05.039 PMID: 32559442

3. Brothers JR, Lohmann Kenneth J. Evidence for Geomagnetic Imprinting and Magnetic Navigation in the Natal Homing of Sea Turtles. Current Biology. 2015; 25(3):392–6. https://doi.org/10.1016/j.cub.2014.12.035 PMID: 25601546

4. Wiltschko R, Wiltschko W. Magnetoreception in birds. J R Soc Interface. 2019; 16(158):20190295–. Epub 2019/09/04. https://doi.org/10.1098/rsif.2019.0295 PMID: 31480921.

5. Benhamou S, Sudre J, Bourjea J, Ciccione S, De Santis A, Luschi P. The role of geomagnetic cues in green turtle open sea navigation. PloS one. 2011; 6(10):e26672–e. Epub 2011/10/26. https://doi.org/10.1371/journal.pone.0026672 PMID: 22046329.

6. Putman NF, Jenkins ES, Michielsens CGJ, Noakes DLG. Geomagnetic imprinting predicts spatio-temporal variation in homing migration of pink and sockeye salmon. J R Soc Interface. 2014; 11 (99):20140542. https://doi.org/10.1098/rsif.2014.0542 PMID: 25056214.

7. Winklhofer M. Magnetoreception: A Dynamo in the Inner Ear of Pigeons. Current Biology. 2019; 29(23): R1224–R6. https://doi.org/10.1016/j.cub.2019.10.022 PMID: 31794751

8. Naisbett-Jones LC, Putman NF, Stephenson JF, Ladak S, Young KA. A Magnetic Map Leads Juvenile European Eels to the Gulf Stream. Current Biology. 2017; 27(8):1236–40. https://doi.org/10.1016/j.cub.2017.03.015 PMID: 28416118

9. Beason RC, Wiltschko R, Wiltschko W. Pigeon homing: Effects of magnetic pulses on initial orientation. The Auk. 1997; 114(3):405–15. PMID: 196467431; 03380385.

10. Wiltschko W, Wiltschko R. Magnetic orientation and magnetoreception in birds and other animals. Journal of Comparative Physiology A. 2005; 191(8):675–93. https://doi.org/10.1007/s00359-005-0627-7 PMID: 15886990

11. Hart V, Kušta T, Němec P, Bláhová V, Ježek M, Nováková P, et al. Magnetic Alignment in Carps: Evidence from the Czech Christmas Fish Market. PloS one. 2012; 7(12):e51100. https://doi.org/10.1371/journal.pone.0051100 PMID: 23227241

12. Brown HR, Ilyinsky OB. The ampullae of Lorenzini in the magnetic field. Journal of comparative physiology. 1978; 126(4):333–41. https://doi.org/10.1007/BF00667103

13. Lissmann KEM H.W. Electric Receptors in a Non-electric Fish (*Clarias*). Nature 1963; 199:88–9. https://doi.org/10.1038/199088a0 PMID: 14047960

14. Wachtel AW, Szamier RB. Special cutaneous receptor organs of fish. IV. Ampullary organs of the non-electric catfish, Kryptopterus. Journal of morphology. 1969; 128(3):291–308. Epub 1969/07/01. https://doi.org/10.1002/jmor.1051280303 PMID: 5798185.

15. Ng HH, Kottelat M. After eighty years of misidentification, a name for the glass catfish (Teleostei: Siluridae). Zootaxa. 2013; 3630:308–16. Epub 2013/01/01. https://doi.org/10.11646/zootaxa.3630.2.6 PMID: 26131513.

16. Rummer JL, Wang S, Steffensen JF, Randall DJ. Function and control of the fish secondary vascular system, a contrast to mammalian lymphatic systems. The Journal of Experimental Biology. 2014; 217 (5):751. https://doi.org/10.1242/jeb.086348 PMID: 24198251

17. Han JE, Choresca CH, Koo OJ, Oh HJ, Hong SG, Kim JH, et al. Establishment of glass catfish (Kryptopterus bicirrhis) fin-derived cells. Cell Biol Int Rep (2010). 2011; 18(1):e00008–e. Epub 2011/03/18. https://doi.org/10.1042/CBR20110002 PMID: 23119145.

18. Bever MM, Borgens RB. Patterning in the regeneration of electroreceptors in the fin of Kryptopterus. Journal of Comparative Neurology. 1991; 309(2):218–30. https://doi.org/10.1002/cne.903090204 PMID: 1885786

19. Struik ML, Steenbergen HG, Koster AS, Bretschneider F, Peters RC. Simultaneous measurements of calcium mobilization and afferent nerve activity in electroreceptor organs of anesthetized Kryptopterus bicirrhis. Comparative Biochemistry and Physiology Part A: Molecular & Integrative Physiology. 2001; 130(3):607–13. https://doi.org/10.1016/s1095-6433(01)00436-6 PMID: 11913470

20. Krishnan V, Park SA, Shin SS, Alon L, Tressler CM, Stokes W, et al. Wireless control of cellular function by activation of a novel protein responsive to electromagnetic fields. Scientific reports. 2018; 8(1):8764. Epub 2018/06/10. https://doi.org/10.1038/s41598-018-27087-9 PMID: 29884813; PubMed Central PMCID: PMC5993716.

21. Hwang J, Choi Y, Lee K, Krishnan V, Pelled G, Gilad AA, et al. Regulation of Electromagnetic Perceptive Gene Using Ferromagnetic Particles for the External Control of Calcium Ion Transport. Biomolecules. 2020; 10(2):308. https://doi.org/10.3390/biom10020308 PMID: 32075263.

22. Cywiak C, Ashbaugh RC, Metto AC, Udpa L, Qian C, Gilad AA, et al. Non-invasive neuromodulation using rTMS and the electromagnetic-perceptive gene (EPG) facilitates plasticity after nerve injury. Brain Stimulation. 2020; 13(6):1774–83. https://doi.org/10.1016/j.brs.2020.10.006 PMID: 33068795

23. Winklhofer M, Kirschvink JL. A quantitative assessment of torque-transducer models for magnetoreception. Journal of The Royal Society Interface. 2010; 7(suppl_2):S273–S89. https://doi.org/10.1098/rsif.2009.0435.focus PMID: 20086054

24. Walker MM. A model for encoding of magnetic field intensity by magnetite-based magnetoreceptor cells. Journal of Theoretical Biology. 2008; 250(1):85–91. https://doi.org/10.1016/j.jtbi.2007.09.030 PMID: 18028964

25. Ritz T, Adem S, Schulten K. A model for photoreceptor-based magnetoreception in birds. Biophys J. 2000; 78(2):707–18. https://doi.org/10.1016/S0006-3495(00)76629-X PMID: 10653784.

26. Gregory NT, Hochstoeger; David, Keays. Magnetoreception-A sense without a receptor. PLoS biology. 2017; 15(10): e2003234. https://doi.org/10.1371/journal.pbio.2003234 PMID: 29059181

27. Hore PJ, Mouritsen H. The Radical-Pair Mechanism of Magnetoreception. Annual review of biophysics. 2016; 45:299–344. Epub 2016/05/25. https://doi.org/10.1146/annurev-biophys-032116-094545 PMID: 27216936.

28. Bernd Fritzsch HS. Evolution of vertebrate mechanosensory hair cells and inne ears: toward identifying stimuli that select mutation driven altered morphologies. J Comp Physiol A Neuroethol Sens Neural Behav physiol. 2015; 200(1):5–18.

29. Eder SH, Gigler AM, Hanzlik M, Winklhofer M. Sub-micrometer-scale mapping of magnetite crystals and sulfur globules in magnetotactic bacteria using confocal Raman micro-spectrometry. PloS one. 2014; 9(9):e107356. Epub 2014/09/19. https://doi.org/10.1371/journal.pone.0107356 PMID: 25233081; PubMed Central PMCID: PMC4169400.

30. Waranyu Khunjaroenrak SP. Embryonic and Larval Development of Glass Catfish *Kryptopterus vitreolus*. Journal Of Argiculture Research and Extension. 2019; 37(1):29–39.

31. London S, Volkoff H. Cloning and effects of fasting on the brain expression levels of appetite-regulators and reproductive hormones in glass catfish (Kryptopterus vitreolus). Comparative Biochemistry and Physiology Part A: Molecular & Integrative Physiology. 2019; 228:94–102. https://doi.org/10.1016/j.cbpa.2018.11.009.

32. Delcourt J, Miller NY, Couzin ID, Garnier S. Methods for the effective study of collective behavior in a radial arm maze. Behavior research methods. 2018; 50(4):1673–85. Epub 2018/02/22. https://doi.org/10.3758/s13428-018-1024-9 PMID: 29464590.

33. Mathis A, Mamidanna P, Cury KM, Abe T, Murthy VN, Mathis MW, et al. DeepLabCut: markerless pose estimation of user-defined body parts with deep learning. Nature Neuroscience. 2018; 21(9):1281–9. https://doi.org/10.1038/s41593-018-0209-y PMID: 30127430

34. Nath T, Mathis A, Chen AC, Patel A, Bethge M, Mathis MW. Using DeepLabCut for 3D markerless pose estimation across species and behaviors. Nature Protocols. 2019; 14(7):2152–76. https://doi.org/10.1038/s41596-019-0176-0 PMID: 31227823

35. Hutchison ZL, Gill AB, Sigray P, He H, King JW. Anthropogenic electromagnetic fields (EMF) influence the behaviour of bottom-dwelling marine species. Scientific reports. 2020; 10(1):4219. Epub 2020/03/08. https://doi.org/10.1038/s41598-020-60793-x PMID: 32144341; PubMed Central PMCID: PMC7060209.

36. Krzysztof Formicki AKO, Adam Tański. Magnetoreception in fish. Journal of Fish Biology. 2019; 95 (1):73–91. https://doi.org/10.1111/jfb.13998 PMID: 31054161

37. Johnsen S, Lohmann KJ. The physics and neurobiology of magnetoreception. Nature Reviews Neuroscience. 2005; 6(9):703–12. https://doi.org/10.1038/nrn1745 PMID: 16100517

38. Lohmann KJ. Magnetic-field perception. Nature. 2010; 464(7292):1140–2. https://doi.org/10.1038/4641140a PMID: 20414302

39. Johnsen S, Lohmann KJ. Magnetoreception in animals. Physics Today. 2008; 61(3):29–35. https://doi.org/10.1063/1.2897947

40. Babineau D, Lewis JE, Longtin A. Spatial acuity and prey detection in weakly electric fish. PLoS Comput Biol. 2007; 3(3):e38–e. https://doi.org/10.1371/journal.pcbi.0030038 PMID: 17335346.

41. Fishelson L, Baranes A. Distribution, morphology, and cytology of ampullae of Lorenzini in the Oman shark, Iago omanensis (Triakidae), from the Gulf of Aqaba, Red Sea. The Anatomical Record. 1998; 251(4):417–30. https://doi.org/10.1002/(SICI)1097-0185(199808)251:4<417::AID-AR1>3.0.CO;2-P PMID: 9713980

42. Manger PR, Pettigrew JD, Fjällbrant TT, Manger PR, Pettigrew JD. Some related aspects of platypus electroreception: temporal integration behaviour, electroreceptive thresholds and directionality of the bill acting as an antenna. Philosophical Transactions of the Royal Society of London Series B: Biological Sciences. 1998; 353(1372):1211–9. https://doi.org/10.1098/rstb.1998.0277 PMID: 9720116

43. Manger PR, Pettigrew JD. Electroreception and the feeding behaviour of platypus (Ornithorhynchus anatinus: Monotremata: Mammalia). Philosophical Transactions of the Royal Society of London Series B: Biological Sciences. 1995; 347(1322):359–81. https://doi.org/10.1098/rstb.1995.0030

44. de Oliveira JF, Wajnberg E, Esquivel DMdS, Weinkauf S, Winklhofer M, Hanzlik M. Ant antennae: are they sites for magnetoreception? J R Soc Interface. 2010; 7(42):143–52. Epub 2009/05/27. https://doi.org/10.1098/rsif.2009.0102 PMID: 19474081.

45. Vidal-Gadea A, Ward K, Beron C, Ghorashian N, Gokce S, Russell J, et al. Magnetosensitive neurons mediate geomagnetic orientation in Caenorhabditis elegans. Elife. 2015; 4:e07493. https://doi.org/10.7554/eLife.07493 PMID: 26083711.

46. Burda H, Begall S, Červený J, Neef J, Němec P. Extremely low-frequency electromagnetic fields disrupt magnetic alignment of ruminants. Proceedings of the National Academy of Sciences. 2009; 106 (14):5708. https://doi.org/10.1073/pnas.0811194106 PMID: 19299504

47. Osipova EA, Pavlova VV, Nepomnyashchikh VA, Krylov VV. Influence of magnetic field on zebrafish activity and orientation in a plus maze. Behavioural Processes. 2016; 122:80–6. https://doi.org/10.1016/j.beproc.2015.11.009 PMID: 26589739